

Concept Paper

Challenges in the Paleoclimatic Evolution of the Arctic and Subarctic Pacific since the Last Glacial Period—The Sino–German Pacific–Arctic Experiment (SiGePAX)

Gerrit Lohmann ^{1,2,3,*} , Lester Lembke-Jene ¹ , Ralf Tiedemann ^{1,3,4}, Xun Gong ¹ , Patrick Scholz ¹ , Jianjun Zou ^{5,6} and Xuefa Shi ^{5,6}

¹ Alfred-Wegener-Institut Helmholtz-Zentrum für Polar- und Meeresforschung Bremerhaven, 27570 Bremerhaven, Germany; Lester.Lembke-Jene@awi.de (L.L.-J.); Ralf.Tiedemann@awi.de (R.T.); GongXun.Allen@awi.de (X.G.); Patrick.Scholz@awi.de (P.S.)

² Department of Environmental Physics, University of Bremen, 28359 Bremen, Germany

³ MARUM Center for Marine Environmental Sciences, University of Bremen, 28359 Bremen, Germany

⁴ Department of Geosciences, University of Bremen, 28359 Bremen, Germany

⁵ First Institute of Oceanography, Ministry of Natural Resources, Qingdao 266061, China; zoujianjun@fio.org.cn (J.Z.); xfshi@fio.org.cn (X.S.)

⁶ Pilot National Laboratory for Marine Science and Technology, Qingdao 266061, China

* Correspondence: Gerrit.Lohmann@awi.de

Received: 24 December 2018; Accepted: 15 January 2019; Published: 24 January 2019



Abstract: Arctic and subarctic regions are sensitive to climate change and, reversely, provide dramatic feedbacks to the global climate. With a focus on discovering paleoclimate and paleoceanographic evolution in the Arctic and Northwest Pacific Oceans during the last 20,000 years, we proposed this German–Sino cooperation program according to the announcement “Federal Ministry of Education and Research (BMBF) of the Federal Republic of Germany for a German–Sino cooperation program in the marine and polar research”. Our proposed program integrates the advantages of the Arctic and Subarctic marine sediment studies in AWI (Alfred Wegener Institute) and FIO (First Institute of Oceanography). For the first time, the collection of sediment cores can cover all climatological key regions in the Arctic and Northwest Pacific Oceans. Furthermore, the climate modeling work at AWI enables a “Data-Model Syntheses”, which are crucial for exploring the underlying mechanisms of observed changes in proxy records.

Keywords: paleoclimate; Pacific Ocean; Arctic climate; paleoclimate data; modeling; data-model comparison; proxy data

1. Introduction

Paleoclimate studies in the Arctic and Subarctic Regions are of vital importance for a better understanding of the natural processes in the climate system that exclude the impacts of human activities. We carry out a German-Sino cooperative research program in marine and polar research which is based on an existing close cooperation in paleoclimate research between the Alfred Wegener Institute, Helmholtz Centre for Polar and Marine Research (AWI, Germany), and the First Institute of Oceanography, Ministry of Natural Resources (FIO, China). In Germany, the program work is carried out by the Paleoclimate Dynamics Group (led by Prof. Dr. Gerrit Lohmann) (AWI), and the Marine Geology Group (led by Prof. Dr. Ralf Tiedemann) (AWI). In China, the cooperation research is going to be undertaken by the Lab of Marine Geology and Geophysics, in FIO (led by Prof. Dr.

Xuefa Shi). All three groups are renowned for their scientific achievements in this field. One visible achievement according to the specified research plan will be the provision of a data basis for a highly productive grid-based platform, which enables efficient proxy and model data processing on an international level. Furthermore, our program also shows large potential in long-term benefits for international cooperation.

2. The Research Area: Modern Ocean–Atmosphere Forcing, Freshwater Flux, Sea Ice Patterns, and Upper Ocean and Intermediate Water Circulation

Today, surface and deeper waters are exchanged between the Arctic Ocean, the subarctic marginal seas and the open North Pacific through the Bering Strait, as well as a series of straits and passages in the Kurile and Aleutian Island chains, respectively [1,2]. New waters mostly enter the marginal seas through large-scale current systems, such as the Alaskan Stream and the East Kamchatka Current (Figure 1).

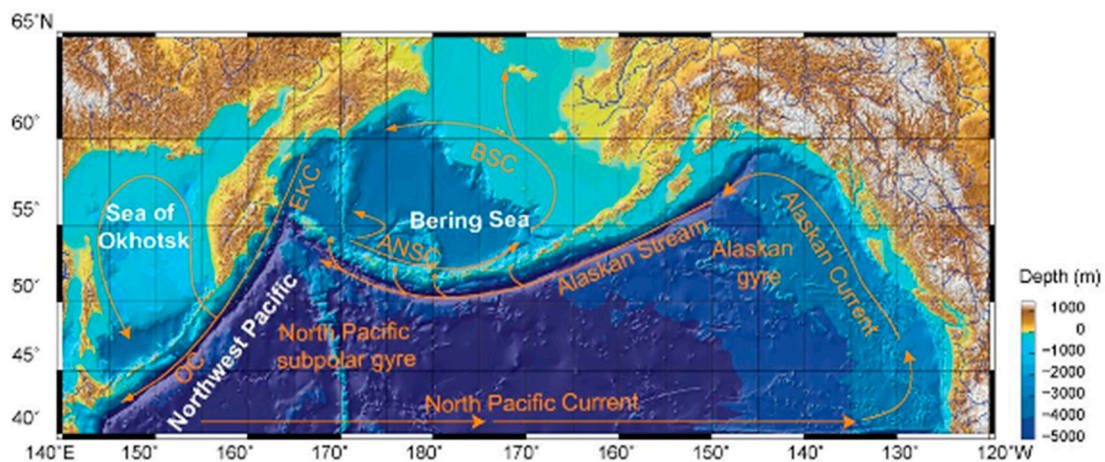


Figure 1. Bathymetric chart of the study region with major oceanic surface currents (orange arrows) from Max et al. [3]. OC = Oyashio Current; EKC = East Kamchatka Current; ANSC = Aleutian North Slope Current; BSC = Bering Slope Current.

The proposed region is linked via teleconnections to both high and low latitude climatic patterns, making it an ideal, highly sensitive candidate to investigate coupling and interaction of major polar and tropical climate mechanisms. The Arctic Oscillation and the strength of the Siberian High/Aleutian Low system in wintertime is one dominant factor for the amount of snow cover and winter strength [4–6], including the timing of sea ice onset and breakup (cf. Figure 2) [7]. These systems provide a link between the high northern latitudes in the Atlantic and Pacific realm. The East Asian Summer Monsoon system, on the other hand, delivers precipitation and heat from the tropics during the summer to the extratropical North Pacific and the continental hinterland major river catchment areas [8–10]. These fluctuations in freshwater discharge, in turn, play an active role in controlling sea ice formation and upper ocean hydrography [11].

In addition to these upper ocean and atmospheric components, the North Pacific Ocean is the terminus of the global Meridional Overturning Circulation. No new deep-water masses are formed [12,13], and the deep North Pacific harbors the oldest and most CO₂-enriched water masses in the modern world ocean [14,15].

Only the mid-depth (500–1000 m) water layer in the North Pacific is replenished and ventilated by newly formed North Pacific Intermediate Water (Figure 3, abbr. NPIW), which is largely determined by precursor water masses from the subarctic marginal seas [16,17], mainly the Okhotsk Sea and, to a lesser extent, Bering Sea and Alaskan Gyre [16,18,19]. Residence and formation times of these mid-depth waters are short and range between one and four years [1]. These fast response times make NPIW especially sensitive to anthropogenic global climate change on short, human timescales,

as indicated by recent instrumental studies that show warming, freshening, and de-oxygenation in North Pacific mid-depth waters over the past ca. 50 years [20–23].

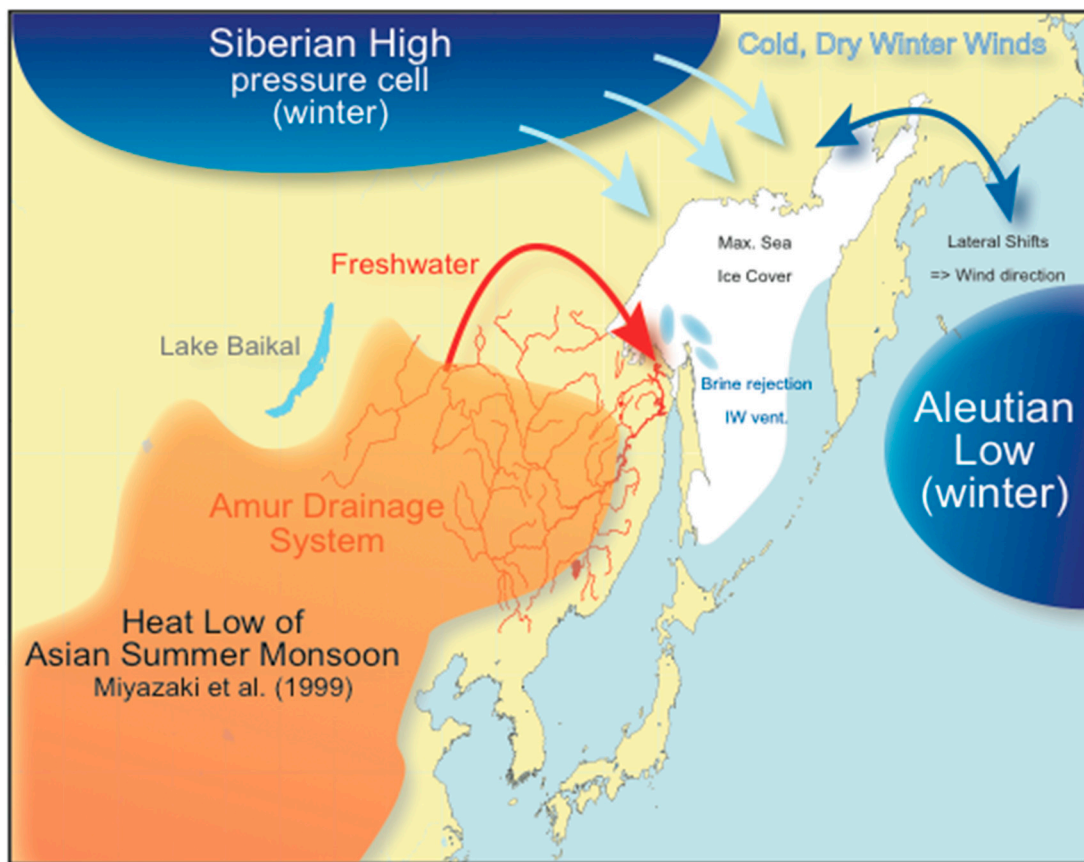


Figure 2. Schematic overview of forcing factors in the study area that influence sea surface temperatures and salinities, as well as mixed layer dynamics. This, in turn, determines the formation and ventilation rates of intermediate waters and the Pacific Meridional Overturning Circulation.

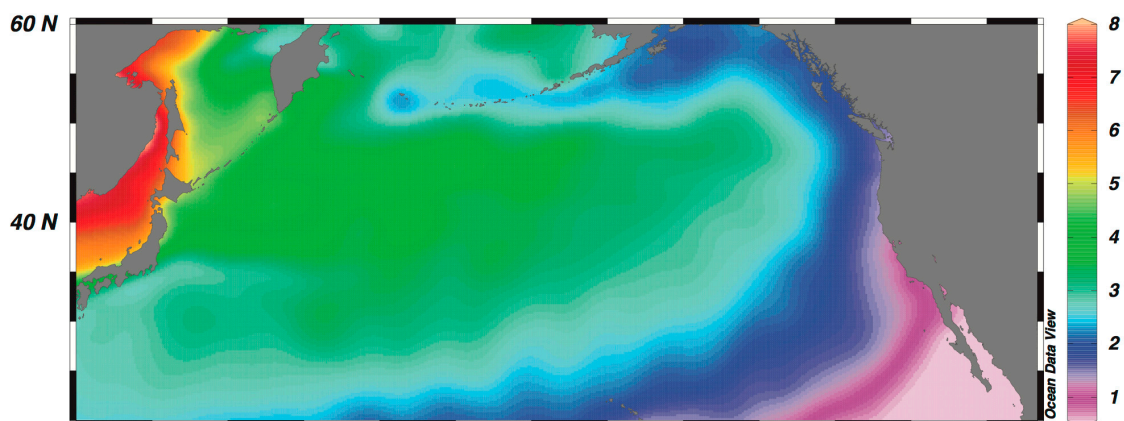


Figure 3. Ventilation characteristics of North Pacific mid-depth water masses, as evidenced by oxygen concentration in mL/L on density surface 26.8 kg/m^3 . Note the source of well-ventilated North Pacific Intermediate Water (NPIW) in the Okhotsk Sea due to brine rejection-induced ventilation processes during the wintertime sea ice season. Data from World Ocean Atlas 2009 [24]. This section may be divided by subheadings. It should provide a concise and precise description of the experimental results, their interpretation, as well as the experimental conclusions that can be drawn.

3. State of Scientific Knowledge and Hypotheses

Paleoceanographic proxy-based and modeling research in the subarctic North Pacific, the Bering Sea, and the Okhotsk Sea has intensified over the past decades and increasingly moved to studies with higher temporal and spatial resolution, focusing on the interaction between sea ice, productivity and upper ocean stratification [25,26]. In this context, previous works established the understanding of dominant large-scale oceanic and atmospheric controls on changing parameters in the Okhotsk Sea [27–29]. For the last million years, *Nürnberg and Tiedemann* [29] first linked changes in primary productivity and sea ice to large orbital-scale climatic variations in SE Asian Monsoon. Subsequent works established that stratification changes induced by sea ice variations and freshwater transport in combination with glacial/interglacial sea level changes constitute control mechanisms for primary productivity changes, peaking during glacial terminations. These works have in addition targeted the detection and analysis of millennial-scale variations in sea ice coverage and productivity, often during the glacial period [28,30–32]. Specific outcomes and resulting contributions by the two working groups to the present state of knowledge, and scientific hypotheses directly related to this project, are discussed hereafter.

In turn, the complementary simulation of the different components of the Earth's system in various climate stages puts increasing emphasis is on the large-scale circulation and data-model comparison (e.g., [33–35]). For the North Atlantic realm, instrumental data, model results, and proxy data have been used to obtain information about the present and past climate teleconnections, Another emphasis is on the large-scale circulation in relation to the hydrological cycle, the deglaciation [33–39], and data-model comparison [40–46]. Instrumental and proxy data have been used to obtain information about present and past climate modes [45,47–51]. A recent focus is put on isotopes for various climate stages [52–57].

3.1. The Pacific Overturning Circulation and Carbon Budget during the Last Glacial

Glacial deep-to-intermediate ventilation boundaries and carbon exchange in the Pacific have fundamental implications for the glacial global carbon budget and the storage of abyssal carbon in the deep ocean [14,15,58,59]. However, evidence from the North Pacific about past variations in glacial NPIW characteristics is still sparse more than a decade after early studies by Mix et al. [60], Zahn et al. [61], and Keigwin [62]. During glacial phases, the closure of the Bering Strait severely restricts the Pacific–Arctic flow, thus changing the circulation and water transport between ocean basins on a hemispheric scale. Some studies (e.g., [63]) suggest that the formation of glacial NPIW mainly occurred in the Bering Sea, in contrast to modern patterns and earlier works [62]. In contrast, several studies show that the Okhotsk Sea remains a source region for intermediate waters (Figure 4). Based on time slice reconstructions from existing sediment cores, datasets from the Okhotsk Sea provide an LGM time slice of the North Pacific ventilation and circulation dynamics based on epibenthic $\delta^{13}\text{C}$ and radiocarbon ventilation ages that can be integrated into earlier works [62,64,65] and lead, together with additional analytical efforts such as determination of paleo-ventilation ages, to a substantially updated synoptic reconstruction of the last glacial Pacific circulation and ventilation.

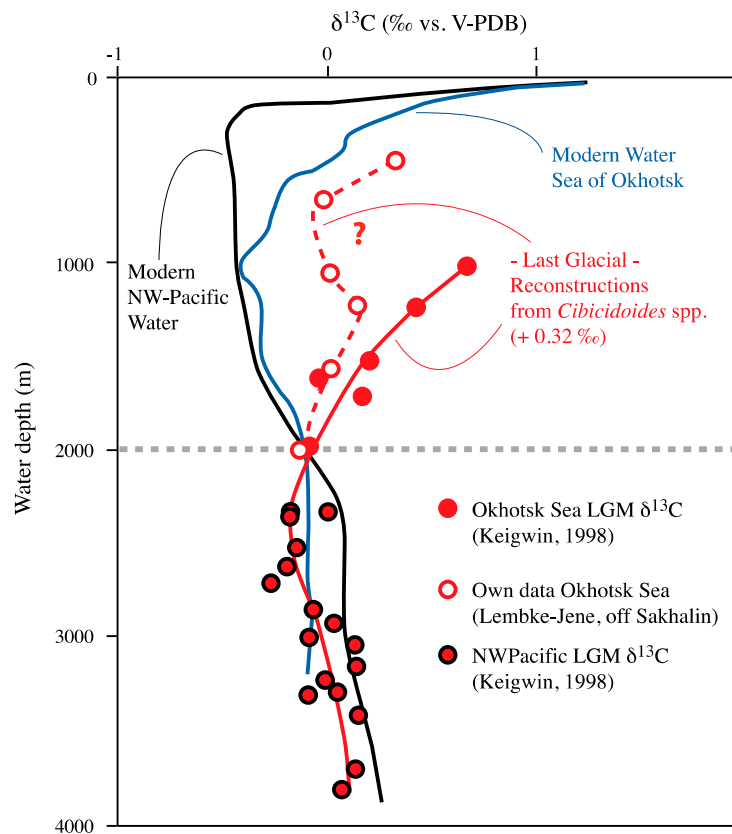


Figure 4. Last Glacial Maximum $\delta^{13}\text{C}$ -based North Pacific depth transect indicative of ventilation patterns. Measurements are based on cores that were retrieved between 1992 and 2004 on a number of subsequent expeditions to the Okhotsk Sea under the frameworks of joint bilateral projects KOMEX, KOMEX II, and KOMEX-SONNE, here shown in comparison to existing data from the Okhotsk Sea and Northwest Pacific [62]. Red open circles denote own unpublished results from water depths between 500 and 2000 m. Filled red circles indicate measurements carried out by Keigwin [62]. Blue solid line shows modern $\delta^{13}\text{C}$ of dissolved inorganic carbon in the Okhotsk Sea, and black lines in the open North Pacific. The results indicate that a previously inferred hydrographic boundary along 2000 m water depth, separating the glacial deep from the mid-depth subarctic North Pacific Ocean probably did not exist in terms of large ventilation differences.

3.2. The Last Glacial Termination in the Subarctic North Pacific

During the deglaciation, the North Pacific underwent drastic and rapid changes in surface and deep circulation and ventilation [26,66–68]. These variations are closely linked to fundamental and rapid changes in the utilization of nutrients [69,70], as well as in surface and deep oceanography [71–73]. For cold Heinrich Stadial 1 (HS-1), widespread convection and the increased formation of new intermediate–deep water masses has been proposed for the North Pacific [68], although newer evidence, based both on model results [74] and data directly from deep sites, alternatively suggest that a potential Pacific overturning cell did not extend beyond 1300–1400 m water depth [75]. This early deglacial episode of better ventilation is sharply contrasted by subsequent oxygen decreases in intermediate water depths and the deposition of laminated sediments along wide swaths of the Pacific coast, including the Bering Sea during the Bølling/Allerød (B/A; 14.6–11.7 kyr BP) (kyr BP: kilo years before present) and the earliest Holocene [76].

Reduced or ceased ventilation of NPIW has been proposed to explain the unusually severe and widespread O_2 -depletion of intermediate waters during the B/A and Preboreal across the North Pacific (e.g., [77]). Alternatively, increases in export production have been invoked as the cause for O_2 depletion through changes in mid-depth remineralization [78]. Lam et al. [79] recently speculated

that transient upper ocean changes in stratification and mixed layer dynamics caused these biogenic productivity peaks.

Own (G. Lohmann) numerical experiments of Heinrich events show that the North Pacific experiences significant hydrographic mixed layer changes during different stages of the last glacial period. During HS-1 (Figure 5), the strength of the Aleutian Low becomes enhanced relative to the LGM, and its core area is also larger. Accordingly, the wind stress over the North Pacific is stronger (Figure 5g), and it significantly strengthens the North Pacific subpolar gyre (Figure 5h). Over the Okhotsk Sea, induced by the stronger Aleutian Low, the surface atmosphere is less cooled (Figure 5c), accompanied by less total precipitation (Figure 5a). Consequently, the sea ice coverage in the Okhotsk Sea is reduced (Figure 5b).

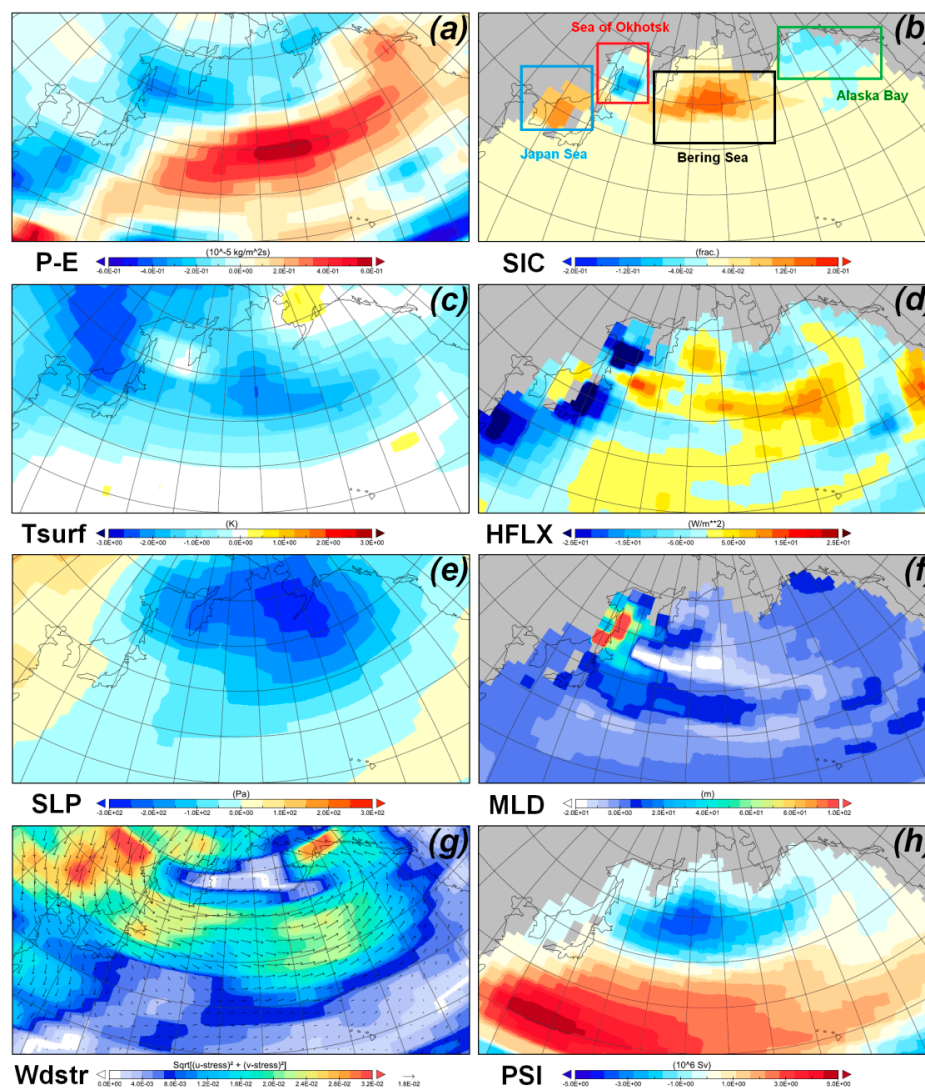


Figure 5. Simulated annual mean surface oceanic and atmospheric anomaly of the Heinrich Event 1 (H1) with respect to the Last Glacial Maximum (LGM). (a) P-E: precipitation minus evaporation, (b) SIC: sea ice concentration, (c) Tsurf: surface atmosphere temperature, (d) HFLUX: total heat flux out of the ocean, (e) SLP: sea level pressures, (f) MLD: mixed-layer depth, (g) Wdstr: wind stress, and (h) PSI: horizontal stream function. Units are given in the color-coded bars below the figures.

Furthermore, a larger area of the open ocean, i.e., without sea ice cover, results in a pronounced oceanic heat loss at the surface (Figure 5d), and prominently deepens the thermocline in the Okhotsk Sea (Figure 5f). In the comparison with the LGM and H1, the climate changes are revealed to be

spatially different in the Japan Sea, Okhotsk Sea, Bering Sea, and the Alaska Bay. Our experiments suggest a prominent role of the Northwest Pacific Ocean during the last deglaciation, especially for the NPIW formation. The exact mechanisms will be explored in this project.

These model-based new inferences are reflected in recent published works that gave a first regional compilation of both alkenone-based sea surface temperatures (SSTs) and upper mixed layer temperatures and salinities derived from Mg/Ca measurements of planktic foraminifera [30]. Results point to a spatially complex regionalized pattern of upper ocean temperature and salinity changes during the last glacial termination (Figure 6) and showed indications for a stronger (weaker) stratification during warmer (colder) millennial-scale climatic changes.

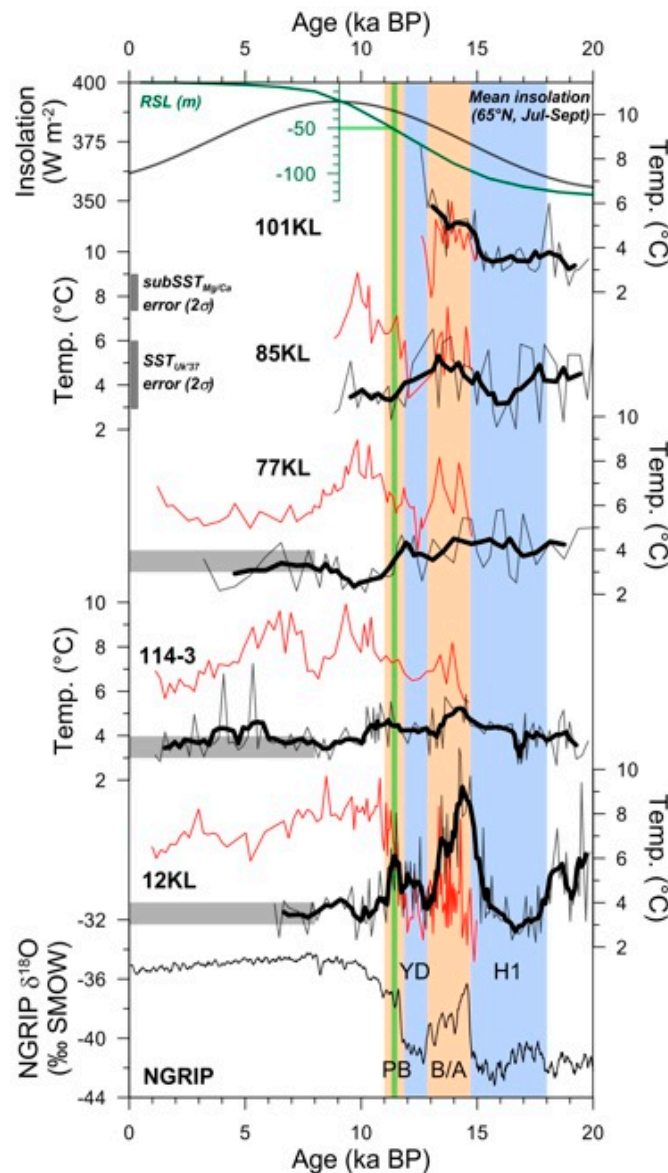


Figure 6. (left panel) Temperature reconstructions covering the last 20 ka from the Bering Sea, the Okhotsk Sea, and the subarctic North Pacific. Northern Greenland Ice Core (NGRIP) oxygen isotope record shown for reference [80]. The sea surface temperature (SST) Mg/Ca records (grey, moving averages in black) are compared to UK'37-based SST data (red), [81]. Shaded areas are averaged mid-Holocene (<8 ka BP) temperatures of 3–4 °C, corresponding to modern temperatures. Sea level curve after [82], vertical green line marks the 50 m sill depth for the Bering Strait. Bølling/Allerød (B/A), Preboreal (PB), Heinrich Stadial 1 (HS-1), and Younger Dryas (YD) marked by colored bars. Figure from Riethdorf et al., 2013 [30].

3.3. Upper Ocean Variability during the Present Holocene Warm Period

Recently, we compared the ocean temperature evolution of the Holocene as simulated by climate models and reconstructed from marine temperature proxies on a global scale [51]. We used transient simulations from a coupled atmosphere–ocean general circulation model, as well as an ensemble of time slice simulations from the Paleoclimate Modelling Intercomparison Project. The proxy dataset comprises a global compilation of marine alkenone- and Mg/Ca-derived SST estimates. Independently of the choice of the climate model, we observe significant mismatches between modeled and estimated SST amplitudes in the trends for the last 6000 years. Alkenone-based SST records show a similar pattern as the simulated annual mean SSTs, but the simulated SST trends underestimate the alkenone-based SST trends by a factor of two to five. We tested if such discrepancies can be caused by too simplistic interpretations of the proxy data [51]. Also, we explored whether the consideration of different growing seasons and depth habitats of the planktonic organisms used for temperature reconstruction could lead to a better agreement of model results with proxy data on a regional scale.

We found that invoking shifts in the living season and habitat depth can remove some of the model–data discrepancies in SST trends [51]. Regardless whether such adjustments in the environmental parameters during the Holocene are realistic, they indicate that when modeled temperature trends are set up to allow drastic shifts in the ecological behavior of planktonic organisms, they do not capture the full range of reconstructed SST trends. Our results indicate that modeled and reconstructed temperature trends are, to a large degree, only qualitatively comparable, thus providing, at present, a challenge for the interpretation of proxy data as well as the model sensitivity to orbital forcing that we want to address with this proposed study. One possible drawback of present climate models is that they cannot represent spatially heterogeneous patterns and regional dynamics. We expect that our new ocean model, which has high resolution in the key areas of the NW Pacific, exhibits a higher sensitivity to external forcing. A logical step is the application of this model to the Holocene, as well as glacial dynamics, to elaborate the local features with potential large-scale implications.

On a regional scale, one of our earlier hypotheses [40] suggested a Holocene SST seesaw pattern between the N-Pacific and N-Atlantic. Based on modeling and limited SST records, a long-term warming of the North Pacific Ocean during the past 7 ka was proposed, whereas the North Atlantic experienced continuous cooling. It was hypothesized that such seesaw pattern is connected to an atmospheric circulation field that comprises elements of the Pacific North American oscillation (PNA) and the North Atlantic Oscillation (NAO) in opposite phases. However, our new initial proxy-based results so far (Figure 7) revealed a spatially diverse SST pattern in the subarctic North Pacific, not supporting the hypothesis of a large-scale Holocene seesaw trend in SST development. All proxy data that are available to date from the entire North Pacific region remain insufficient both in terms of lateral and temporal coverage. Thus, our proposed project will address this shortcoming by establishing a dense network of SST reconstructions to allow for resolving the potentially regional-scale heterogeneous SST evolution. Alkenone-based SST reconstructions will be compared to other proxies (Mg/Ca, TEX86) in order to understand differences in different datasets and assess larger common trends while retaining the chance to better understand the incorporation mechanisms of temperature signals into different methods.

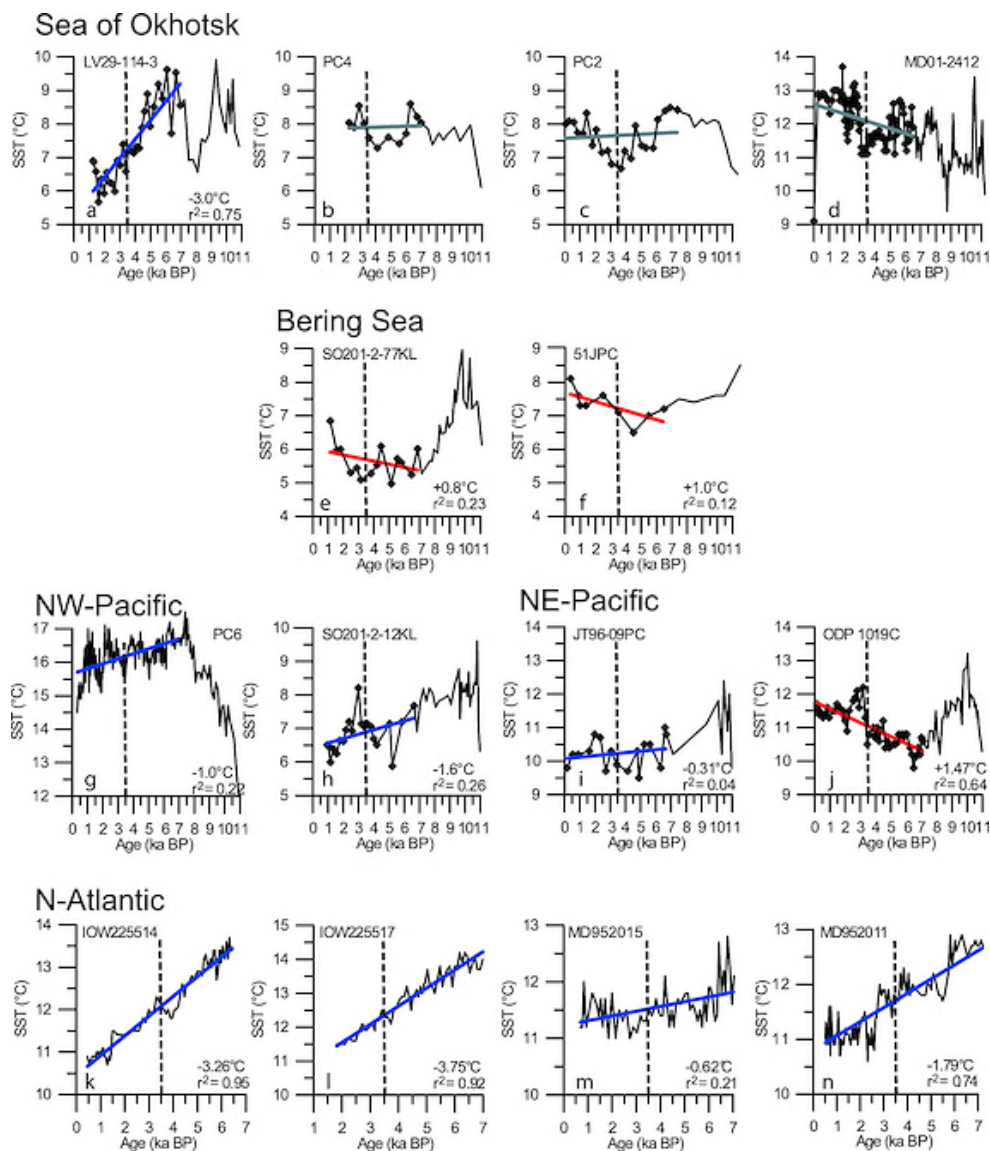


Figure 7. Compilation of alkenone-based SST reconstructions from the North Pacific region ordered according to source for the Holocene period. Lines indicate linear regressions over the last 8 ka, blue = cooling trend, red = warming trend [81].

4. Future Research Targets and Priority Questions

Within the research proposal, we will identify the patterns and amplitudes of natural climate variations on interannual to millennial timescales, with a focus onto the NW Pacific. Through a combination of paleoclimate records from the NW Pacific with the analysis of climate model simulations, we will contribute to a better understanding of the long-term evolution of climate modes and their linkage to regional NW Pacific and large-scale variability. The results will enable us to address the following specific questions:

How well can changes between glacial and interglacial climate variability be quantified and interpreted through a combined model–data approach?

- Do different proxies record the same or different ocean temperature signals?
- How precisely can model outputs and proxy-based datasets be reconciled, or existing offsets mechanistically explained?

- Do proxy data and model result differences change in magnitude and patterns between glacial and interglacial climate states?

What is the response of the atmosphere–ocean circulation in the NW Pacific to deglacial hemispheric warming (onset of B/A and Preboreal) and cooling (HS-1, YD)?

- How do temperature and salinity of the ocean surface and upper mixed layer change in the subarctic North Pacific over the last glacial termination?
- Can potential causes for deglacial changes in upper ocean characteristics be identified in model runs and lead to better constraints on dominant forcing factors?
- Are there regional variations in these upper ocean temperature and salinity characteristics between the open subarctic North Pacific and the neighboring marginal seas?
- What is the rate of changes during the most abrupt climate events during deglaciation?

How and why did surface and mid-depth oceanography and sea ice patterns change during the current “stable warm-house” Holocene?

- How are Holocene climatic changes reflected in our extratropical and subarctic upper ocean and atmosphere model and proxy results?
- Can we discriminate between dominant low and high-latitude forcing mechanisms for North Pacific climate variability that shape Holocene subarctic North Pacific hydrography and biogeochemistry on millennial timescales?
- How does the ventilation of North Pacific Intermediate Water respond to surface ocean and sea ice changes?
- How sensitive is the mid-depth water ventilation process to past higher-than-present temperatures and freshwater fluxes, and to potential millennial-scale warm and cold phases within a warm (Holocene) background climate?
- How well do large-scale detailed regional reconstructions of upper ocean temperature and stratification, in connection with high-resolution models used in this project, help to evaluate and constrain existing hypotheses about climate teleconnections and forcing between the North Atlantic and Pacific?

How sensitive is the sea ice cover in the extra-tropical marginal seas of the North Pacific Ocean and the Arctic Ocean to global environmental changes?

- How well can we compare FESOM model results with quantitative reconstructions of sea ice cover changes on glacial/interglacial and millennial timescales, including differences in distribution between different basins with the existing proxy methods (IP₂₅, transfer functions based on biological proxies)?
- Are deglacial changes in sea surface temperatures and mid-depth ventilation characterized by concomitant changes in sea ice distributions?
- How did sea ice patterns change during warmer-than-present early Holocene climatic boundary conditions?
- Did these climates yield complete loss of sea ice?
- How large are model–data discrepancies?

How did the deglacial opening of the Bering Strait influence the Arctic and North Pacific Ocean paleoceanography and climate?

- How did the meridional overturning circulation (MOC) look when the closed glacial Bering Strait hindered the exchange of freshwater between ocean basins?
- Sensitivity experiments with explicit modeled effect of the Bering Strait throughflow: HS-1 with a closed strait is contrasted to Preboreal conditions with an open strait. It is assumed that an

open Bering Strait provides oceanic connections between the Atlantic Ocean and North Pacific hydrography. This gateway effect shall be separated from the effects of the hydrological cycle and the formation of sea ice. Comparative proxy series from the cores on both sides of the Bering Strait will allow reconstructing the hydrographic influence and changing SST, mixed layer depth and salinity gradients between both ocean basins.

5. Conceptual Approach for Future Work

We aim at further developing the scientific basis for the Arctic–Subarctic climate change and variability on various spatiotemporal scales through further exploration of underlying physic processes. This topic lies within the broad context of paleoclimatic evolution since the last glacial at high latitudes. We, here, for the first time, anticipate to broaden the state of knowledge from “single-site” or locally centered previous works on a national scale into a regional-hemispheric scale synoptic assessment of sea ice, upper ocean, and mid-depth ventilation changes, based on analyses of sediment cores from the Okhotsk and Bering Seas, and the open North Pacific and Arctic Ocean. We regard these under-investigated large regions as key areas for understanding the hemispheric climatic evolutions of the LGM, the last glacial termination, and selected Holocene intervals.

Arctic and Subarctic paleoclimate research and corresponding research approaches in this program have been part of the current work at AWI and FIO. So far, more than 65 FIO high-quality sediment cores have been collected and completely cover climatic key regions in the Arctic and Northwest Pacific Ocean, in connection with more than 110 German sediment cores and corresponding data collections (Figure 8). In addition, based on the available Chinese datasets, this program has a high potential to involve other valuable data resources. With respect to the current situation at AWI and FIO, this bilateral cooperation is proposed based on two advantages:

- Combination of high-resolution and long-period marine records at AWI and FIO that, for the first time, effectively cover all key areas for quantifying Arctic–Subarctic climate changes.
- The climate modeling work in AWI makes it possible to integrate the important data-model syntheses aspect into this bilateral cooperation.

5.1. Proxy Data-Based Paleoceanographic Reconstructions

The objective is to characterize the nature of the surface and deep ocean circulation, upper ocean stratification, sea ice extent, and the resulting hydrographic conditions in the Arctic and NW Pacific Ocean, in particular, in the subarctic marginal seas from the LGM to the pre-industrial (PI) with quantitative proxies.

One focus will be to reconstruct changes in upper ocean temperatures and salinity by a combined approach, using multi-species Mg/Ca ratios and $\delta^{18}\text{O}$ measurements of planktic foraminifera, combined with alkenone-derived SSTs. Both approaches have been used in the study region successfully over these time intervals proposed here [3,30,81]. We broaden the previous approaches by extending the usual single-species planktic foraminifera measurements to an additional species with well-defined calcification depth and seasonal habitat preferences [83–86]: *Neogloboquadrina pachyderma* (sinistral) as the most abundant species is a mixed layer dweller with a preference to settle near the temperature minimum and pycnocline (80–200 m, cf. [87]), whereas *Globigerina bulloides*, an opportunistic phytodetritus feeder, prefers a shallower to intermediate habitat depth (50–100 m) and often reaches abundance maxima during the high organic matter flux in early spring with the onset of diatom blooms. With this combined approach, we aim to better resolve mixed layer dynamics in temperature and salinity than previously possible, and pave the way for interproxy comparison with alkenone-derived SST reconstructions, which represent the upper 50 m of the water column during the late summer maximum seasonal flux of coccolithophores.

Organic geochemistry samples processed for alkenone-based paleothermometry can, in a second step, be used to determine IP₂₅ concentrations, a new method established at the AWI that allows reconstructing sea ice cover quantitatively, and has been used by us before for data-model

comparisons [88,89]. These geochemistry-based reconstructions of paleo-sea ice cover will be validated by a smaller number of samples, on which micropaleontological works by collaborators allow for development of alternative multi-proxy sea ice reconstructions based on microfossil assemblages via transfer function and modern analog techniques [90].

Taken together, the findings from these surface and upper ocean proxies are instrumental to understanding the role that SST, stratification, and sea ice changes exert on the ventilation and circulation of deeper water masses. For reconstructions of the circulation and formation of deep and intermediate waters we will use stable isotopes of epibenthic foraminifera, in conjunction with AMS ^{14}C values, as tracers for water mass ages. On selected time intervals and sites, we will combine those “standard data” (which are also planned to be generated directly from model runs for comparisons) with proxies for paleo-circulation dynamics, such as sortable silt size and Pd/Th measurements, to help disentangle evidence of the paleo-chemical (nutrient recycling, biological pumping) from the paleo-physical component (water mass transport). With this approach, we plan to facilitate a better setup for synthesis works and direct comparisons between proxy timeseries and modeling results.

To achieve a sufficient coverage of the study area to enable the data-model comparisons envisioned here, we will be analyzing a high number (>50) of sediment records within the joint German-Sino collaboration proposed here (cf. core sites Figure 8). We plan to utilize the full range of available sediment core materials from both partners, including earlier legacy cores from predecessor BMBF-funded program activities in the Okhotsk Sea (KOMEX I and II, KOMEX SO178), and the North Pacific (INOPEX) and Bering Sea (KALMAR and INOPEX). Regarding sample selection, we will follow a tiered approach in line with the modeling setup described above.

To complete a regional validation of the used proxies and a calibration of data-model-instrument test, we start by establishing a network of surface sediment or modern samples. Taken together, the sample number should range between 50 and 100, depending on the quality and availability of material. Results from these analyses will be directly compared to instrumental or re-analysis datasets, and checked against the modern or PI model run.

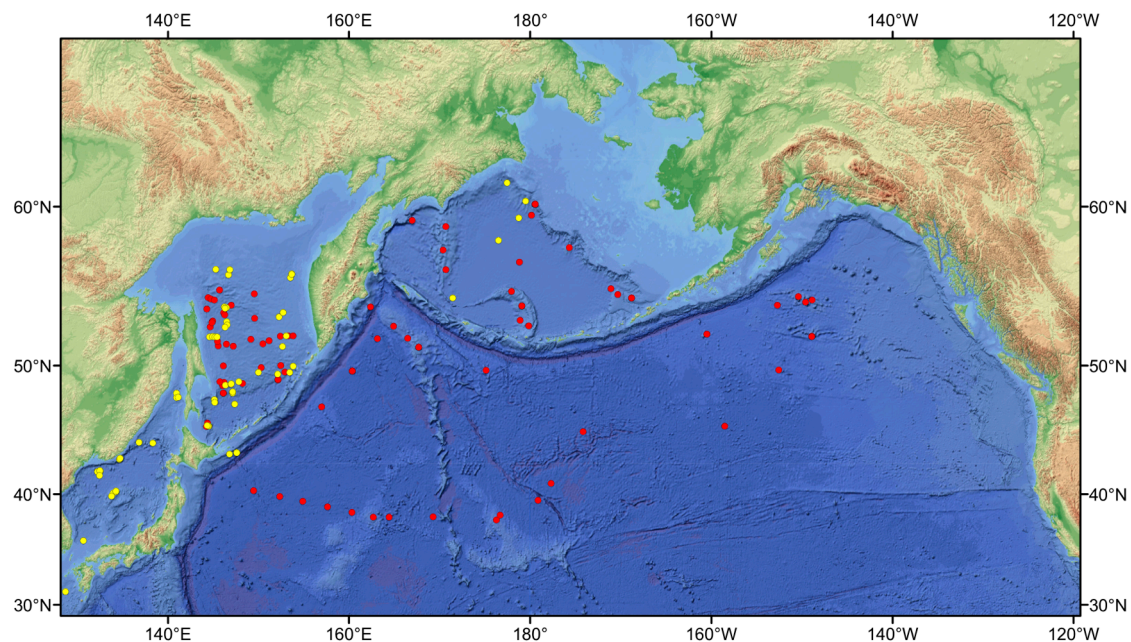


Figure 8. Sino–German Network of sites with high-quality sediment cores in the subarctic Pacific. German sediment coring campaigns in red (KOMEX I and II, KOMEX-SO178, KALMAR, INOPEX), and Chinese FIO sediment cores in yellow. For orientation, the water depth is shown as bluish colors.

Based on these initial works on modern settings, we set out in close collaboration with our Chinese partners to develop a comprehensive stratigraphic framework based on lithostratigraphic

correlation through various core logging and scanning techniques (shipboard color, physical properties and magnetic susceptibility data, shore-based high-resolution XRF scanning). This framework will be anchored in absolute ages with a suite of AMS ^{14}C dates on planktic foraminifera from jointly defined key sites. Based on the stratigraphic context and the joint initial assessment, we will select the appropriate cores for further investigations of the defined time slices (PI, 6 ka, 9 ka, LGM) and the time periods of transient model runs (within the 8–18 ka period). Taken together, the findings from these surface and upper ocean proxies are instrumental to understanding the role that the subarctic Pacific played in the global MOC and past Northern Hemisphere climate.

5.2. Paleoclimate Modeling: Numerical Simulations

The objective of such works is to provide reliable physical hypotheses to interpret paleoclimate records in spatiotemporal dimensions, and aims to explore the mechanisms behind these paleoclimate reconstructions. The numerical approach complements the reconstruction approach of proxy data to gain a better understanding of the individual components and processes in the Earth's complex climate system. The NW Pacific shows a pronounced sensitivity and heterogeneity to climate changes and variability under a global view (Figure 5), the Arctic and Subarctic regions are also characterized with complicated bathymetry map and land sea mask, especially during the last glacial period. We will apply a state-of-the-art Earth System Model (ESM) and a Finite Element Sea Ice–Ocean Model (FESOM).

The ESM is a fully coupled ocean–atmosphere–sea ice–land surface model [91]. Our version has been applied and tested for the Cenozoic climate [92–94] and glacial [95,96] and interglacial climate states [97,98]. The ocean component is the ocean general circulation model MPIOM, utilizing a curvilinear Arakawa-C grid with a formal horizontal resolution of $\sim 3^\circ \times 1.8^\circ$ and 40 uneven vertical layers, including the dynamics of sea ice formulated by viscous–plastic rheology [99]. The atmospheric component, ECHAM5, runs at a horizontal resolution of $\sim 3.75^\circ \times 3.75^\circ$ with 19 vertical levels, and is complemented by the land surface scheme JSBACH including a dynamical vegetation module.

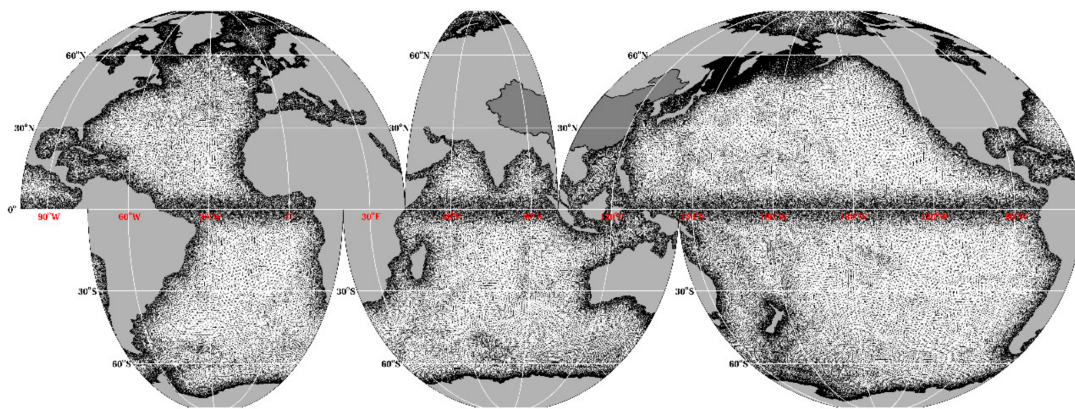
In the following, the planned model scenarios are described:

1. To conduct transit ESM simulations from the late glacial to the B/A period, with orbital forcing (16.8–12.7 ka) and prescribed glacial/interglacial land ice distributions.
2. Using the ESM version including the ice sheets, a transient experiment from the HS-1 to B/A onset with prescribed and fully interactive ice sheets will be performed. These experiments are established to understand abrupt climate changes during the last deglaciation, especially as the subarctic Pacific climate system has been demonstrated to be sensitive to the sea level changes. This experiment is conducted based on the simulation results of 1.
3. To conduct experiments using the isotope-enabled version including the marine carbon industry and oxygen isotope cycle modules, aiming for a direct comparison with proxy reconstructions (C-13; C-14; O-18).

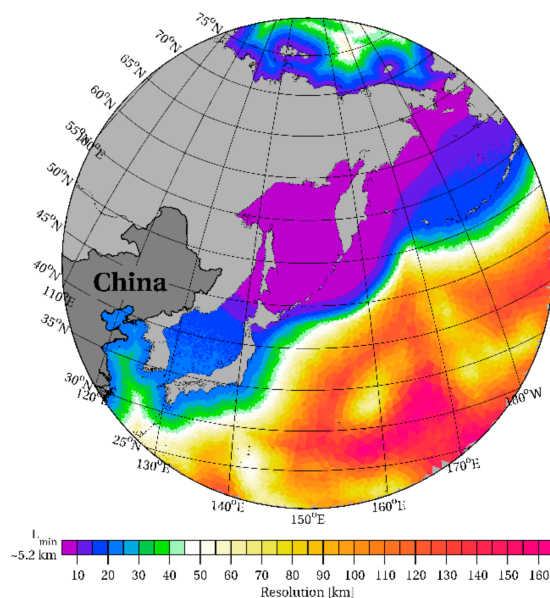
The second model in the proposed work is the coupled Finite Element Sea Ice–Ocean Model (FESOM) developed at Alfred Wegener Institute (AWI). FESOM is a convenient approach to study a broad range of spatial scales by using an unstructured triangular surface mesh which provides the opportunity to highly resolve coast lines and areas of interest in a coarser global setup without complicated grid nesting (see Scholz et al. [100] for a “North Atlantic setup”). FESOM works with tetrahedral 3D elements and consists of the Finite Element Ocean Model (FEOM) coupled to a Finite Element dynamic thermodynamic Sea Ice Model. The Sea Ice and the Ocean models share the same triangular surface mesh. The setup of FESOM requests massive parallel computational facilities such as the North-German Supercomputing Alliance.

FESOM is able to capture sufficient details in the regions of interest where the dynamics have small spatial scales (the Bering Sea, Okhotsk Sea, and Chukchi Sea) within a global scope (Figures 5 and 9). For the objective target of simulating the variability in sea ice coverage, ocean circulation, and hydrology in the marginal seas of the NW Pacific on a highly resolved regional scale in an otherwise

coarser global setup, we created a customized regional refined FESOM mesh, shown in Figure 9. In this proposal, we will highly benefit from FESOM's ability to achieve an eddy-resolving resolution in areas of interest and still keep the computational costs in moderate order, compared to ocean circulation models where high resolution is applied globally. FESOM will allow us to study regional mechanisms, such as eddy interaction with boundary currents and eddy-induced convective plums that contribute to the vertical ventilation of the Northwest Pacific. With FESOM, we will be able to simulate an appropriate in- and outflow of the Okhotsk Sea through the complicated bathymetry structure at the Kurile Island chain.



(a)



(b)

Figure 9. (a) Unstructured triangular Finite Element Sea Ice–Ocean Model (FESOM) surface mesh used in this project, with increased resolution along the bathymetric slope, as well as along the equator. (b) Zoom into the locally refined Sea of Okhotsk and Sea of Japan (up to 7 km resolution). For details of the model, we refer to Scholz et al. [100].

To reach our scientific goals, the strategies of implementing ESM and FESOM modeling work are as follows:

- To conduct simulations with the ESM for the time periods of important climate events during the last glacial periods, e.g., LGM, HS-1, B/A onset, Early Holocene, Mid Holocene, and PI, by changing orbital forcing and prescribed land ice distributions.
- Sensitivity experiments are expected to specify the role of different components in the Earth system.
- To conduct FESOM simulations for detailed ocean circulation changes in the Arctic and subarctic Pacific Oceans (dynamical downscaling of the ocean–sea ice system).
- To perform different time slice experiments under present day, PI, 6 ka, and LGM climate conditions (atmospheric forcing from the ESM). The FESOM model configuration (see Figure 9) will be used to simulate the present day, PI, and 6 ka time slice. The simulation of the LGM conditions requires the design of a further FESOM mesh configuration with a different land–sea mask, due to the sea level being 120 m lower compared to present day. This mesh configuration will be used for sensitivity experiments for the B/A and HS-1.

So far, the ESM and FESOM models have been maturely used in AWI. The ESM version “COSMOS-landveg r2413, 2009” is going to be commonly used for all runs, aiming to achieve the modeling results excluding influences from different model setups. In comparison, FESOM is applied to reveal the details of ocean circulation in a selected area with respect to their background climate conditions. Thus, the choice of FESOM grid can be experiment-dependent. For instance, with the focus on Japan Sea and Sea of Okhotsk, the highest resolution ($<10 \text{ km} \times 10 \text{ km}$) is implemented in the corresponding areas, as shown in Figure 9.

5.3. Proxy Data Syntheses and Data-Model Comparisons

The results from a complementary approach, as described above, will provide a rigorous description of the paleoclimatic evolution of the Arctic and NW Pacific Oceans in terms of its dynamics and global impact with respect to varying background conditions since the last glacial period. By the end of the project, we will be in a position to place new constraints on our mechanistic understanding of the physical processes behind climate events in these regions.

An improved age model for the NW Pacific Ocean is expected. Based on the age model, the climate evolution in specific oceanic regions and the climatic maps for different climate events will be provided, covering climatic key regions in Arctic and subarctic Pacific Oceans.

In the other aspect, we will explore the following scientific question: Could the consideration of different growing seasons and depth habitats of the planktonic organisms used for temperature reconstruction lead to a better agreement of model results with proxy data on a regional scale? Also, is the extent to which temporal shifts in growing season or vertical shifts in depth habitat able to reduce model–data misfits? In addition, we will detect how model-simulated mixed layer dynamics act as a climate index in comparison with proxy reconstruction. This has been proven to be important to improving climate simulations and understanding model–data misfits [51]. Compared to previous “data-model synthesis” work (e.g., [51,74,101–103]), the advantages of FESOM simulations are emphasized in our work by detailed representation of regional ocean circulation and sea ice cover.

Furthermore, our enhanced-version ESM is capable of simulating biogeochemical cycles, including the carbon cycle and marine sediments, as well as isotopes [55,56,104]. This work will be specifically vital in data-model syntheses where we apply proxy modules as well as empirical-statistical models and data analyses of climate modes. Our effort goes beyond time slice experiments and reduced complexity approaches which have been performed so far [68,105,106].

Due to the necessity to first carry out a regional present-day calibration and inter-laboratory data comparison study to enable the generation of high-quality quantitative proxy data for later data-model syntheses, we anticipate that this aspect will run throughout the entire project period. The synthesis of Chinese and German proxy timeseries will be carried out as the first step to generate a coherent, quality-controlled and comparable dataset. The successor activity and the comparison of paleoclimate and model data can be carried out in a number of ways. The simplest approach is

to subsample the model output fields, picking out data only from those locations and seasons for which paleo-reconstructions exist for comparison. However, before a valid comparison can be made, it must be confirmed that the climate response is being compared on similar spatial and temporal scales. There are two key statistical methods that synchronize the spatial scale of the model simulation and proxy reconstruction. The upscaling technique identifies the underlying large-scale processes, e.g., the teleconnections that control low-frequency variations observed in many proxy records. This is in contrast to the downscaling technique, where large-scale information obtained by an ESM modeling simulation can be “zoomed in” to the smaller scale of proxy climate information on the FESOM grid.

6. Partners

The Alfred Wegener Institute for Polar and Marine Research is the national German center for polar research and one of the major German marine research institutions, with a focus on high-latitude areas. It therefore takes a unique position compared to other German research institutions working in these fields. Within an interdisciplinary research environment, AWI personnel study the natural variability of the climate system from short to long timescales. The Arctic is, climatologically, one of the most sensitive regions in the Earth System to anthropogenic climate change and, in this context, it contains valuable sources of information about possible future global environmental change and its consequences. As part of the institutional research programs, key data are obtained on the present-day variability of ocean systems, on climate records with their historic variability in the recent geological past, and on reconstructions of climate history. As the national polar research institute, the AWI is well connected to the international polar research community, has formed numerous alliances with leading polar institutions, and is a partner in, or leading, internationally coordinated research projects. The aims of this program shall be accomplished by two research groups in the AWI:

- The Paleoclimate Dynamics Group (Gerrit Lohmann) is an international team of senior and young scientists coming from different disciplines, such as physics, geosciences, and mathematics. In interdisciplinary research, the group strives to advance the knowledge and understanding of the Earth’s past. The group carries out climate modeling and research in various projects, with both national and international collaborations.
- The Marine Geology Group (Ralf Tiedemann) focuses on the development of a fundamental understanding of Earth’s history and its past evolution. The major research activities are the reconstruction and systematic understanding of past global environmental variability, its mechanisms and impacts, and responses to natural driving forces of climate change. These aims are achieved by interpreting chemical signatures of biologic, oceanographic, and climatic processes that are preserved in the marine sediment record.

The First Institute of Oceanography (FIO), Ministry of Natural Resources, China is a comprehensive oceanographic research institute engaged in applied and basic research, high-technology development, and serving the public. The institute aims at promoting marine science and technology progress, and serving marine management, marine safety, and marine economy development. It thus constitutes an important marine research entity in the national science and technology innovation system. The main research fields at FIO include the distributions and variations of natural environmental elements in Chinese seas and their adjacent oceanic and polar sea areas; marine resources and environmental geology; generating mechanisms and prediction methods of marine disasters; the variability of the marine ecology environment, the remote sensing oceanography, and marine information systems; and the assessment, protection, and regulation of marine environment, marine high-technology development, and marine comprehensive management sciences. In this program, the research work corresponding will be done by the FIO Research Group.

The Key Lab of Marine Resources and Environmental Geology, aims at the development frontiers of international marine geology and major marine geology research, and is engaged in the research of evolution mechanisms of the marine geology environment, also with a focus on high-tech submarine

detection techniques and comprehensive geological information interpretation techniques. In recent years, the laboratory has undertaken many national major thematic projects, national natural science foundation projects, and other geologic survey projects, and has organized the first China oceanic mineral resources surveys. The laboratory has a marine geology sample hall, and has been entrusted to run the China Oceanic Association sample hall. The analytical facilities enable the routine measurements of various proxy data, such as stable and radiogenic isotopes, as well as a broad array of sediment component and geochemical analyses. The laboratory has established good cooperation relations with several countries.

7. Expected Outcome and Dissemination of Results, Benefits for Bilateral Exchange, and Education and Outreach

Based on the anticipated international scope and multidisciplinary nature of the resulting data, additional scientific projects can be expected to result from the project, e.g., in the form of future joint expeditions and strengthened bilateral researcher exchange. This project will provide the basis for a highly productive grid-based platform that enables efficient data processing and German–Sino proxy and model data. AWI is one of the leading partners in these data base initiatives. This project will further improve the current German–Sino cooperation research in marine and polar science, and enhance the bilateral communication and understanding between German and Chinese scientists. Explicitly, within the scope of science, the following long-term benefits can be expected from this project:

- Understanding the Arctic and Northwest Pacific climate system shows the priority in future marine and polar researches. This project will favor the existing advancements of Germany in these fields.
- In addition, Yang et al. [107] demonstrate that climate variation of the East Asia, especially with the Asia winter monsoon, are in close relationship with European climate change.
- In addition, a visible achievement of this program is to provide the basis for a highly productive grid-based platform, which enables efficient proxy and model data processing and exchange between Germany and China. This also establishes a platform for future German–Sino cooperation programs in marine and polar science.

The project thus supplies new data which will be vital for the documentation and understanding of climate development, as well as future climate modeling. These data will be generated from an area which, to date, has only been scarcely focused on, while being nevertheless relevant for local and global climate development. This project is part of a series of national and international research initiatives contributing to the improved understanding of the correlation between climate-driving processes of the low and high northern latitudes and their relation to global climate variability.

Author Contributions: conceptualization, G.L., R.T., X.S., L.L.-J.; software, formal analysis, P.S., X.G.; writing—original draft preparation, G.L., L.L.-J., X.G., P.S., J.Z.; writing—review and editing, L.L.-J., G.L.; supervision, G.L., R.T., X.S.; funding acquisition, G.L., R.T., X.S.

Funding: This proposal was, after positive external peer-review, funded by the German Ministry for Education and Research (BMBF) through grant no. 03F0704A, “WTZ China–SiGePAX”. Further financial support was provided by the National Helmholtz REKLIM Initiative and the Alfred-Wegener-Institut, including the APC.

Acknowledgments: We sincerely thank Stefanie Klebe, Aysel Sorensen, and Katharina Kirchhoff for administrative support, as well as the Projektträger Jülich (PTJ) for helpful comments and assistance.

Conflicts of Interest: The authors declare no conflict of interest. The funders had no role in the design of the study; in the collection, analyses, or interpretation of data; in the writing of the manuscript, or in the decision to publish the results.

References

1. Ohshima, K.I.; Nakanowatari, T.; Riser, S.; Wakatsuchi, M. Seasonal variation in the in- and outflow of the Okhotsk Sea with the North Pacific. *Deep Sea Res. Part II Top. Stud. Oceanogr.* **2010**, *57*, 1247–1256. [[CrossRef](#)]

2. Katsumata, K.; Ohshima, K.I.; Kono, T.; Itoh, M.; Yasuda, I.; Volkov, Y.N.; Wakatsuchi, M. Water exchange and tidal currents through the Bussol' Strait revealed by direct current measurements. *J. Geophys. Res. Oceans* **2004**, *109*, C09S06. [[CrossRef](#)]
3. Max, L. Millennial-Scale Changes in Sea Surface Temperatures and Intermediate Water Circulation in the Northwest Pacific during the Past 20,000 Years. Ph.D. Thesis, University of Bremen, Bremen, Germany, 2012.
4. Rodionov, S.N.; Bond, N.A.; Overland, J.E. The Aleutian Low, storm tracks, and winter climate variability in the Bering Sea. *Deep Sea Res. Part II Top. Stud. Oceanogr.* **2007**, *54*, 2560–2577. [[CrossRef](#)]
5. Overland, J.; Adams, J.; Bond, N. Decadal variability of the Aleutian low and its relation to high-latitude circulation. *J. Clim.* **1999**, *12*, 1542–1548. [[CrossRef](#)]
6. Pickart, R.S.; Moore, G.W.K.; Macdonald, A.M.; Renfrew, I.A.; Walsh, J.E.; Kessler, W.S. Seasonal Evolution of Aleutian Low Pressure Systems: Implications for the North Pacific Subpolar Circulation. *J. Phys. Oceanogr.* **2009**, *39*, 1317–1339. [[CrossRef](#)]
7. Honda, M.; Yamazaki, K.; Tachibana, Y.; Takeuchi, K. Influence of Okhotsk sea-ice extent on atmospheric circulation. *Geophys. Res. Lett.* **1996**, *23*, 3595–3598. [[CrossRef](#)]
8. Ogi, M.; Tachibana, Y. Influence of the annual Arctic Oscillation on the negative correlation between Okhotsk Sea ice and Amur River discharge. *Geophys. Res. Lett.* **2006**, *33*, L08709. [[CrossRef](#)]
9. Ogi, M.; Tachibana, Y.; Yamazaki, K. The connectivity of the winter North Atlantic Oscillation (NAO) and the summer Okhotsk High. *J. Meteorol. Soc. Jpn.* **2004**, *82*, 905–913. [[CrossRef](#)]
10. Tachibana, Y.; Oshima, K.; Ogi, M. Seasonal and interannual variations of Amur River discharge and their relationships to large-scale atmospheric patterns and moisture fluxes. *J. Geophys. Res. Atmos.* **2008**, *113*, D16102. [[CrossRef](#)]
11. Ogi, M.; Tachibana, Y.; Nishio, F.; Danchenkov, M. Does the fresh water supply from the Amur river flowing into the sea of Okhotsk affect sea ice formation? *J. Meteorol. Soc. Jpn.* **2001**, *79*, 123–129. [[CrossRef](#)]
12. Emile-Geay, J.; Cane, M.; Naik, N.; Seager, R.; Clement, A.; Van Geen, A. Warren revisited: Atmospheric freshwater fluxes and “Why is no deep water formed in the North Pacific”. *J. Geophys. Res. Ocean.* **2003**, *108*, 3178. [[CrossRef](#)]
13. Warren, B. Why is no deep water formed in the North Pacific? *J. Mar. Res.* **1983**, *41*, 327–347. [[CrossRef](#)]
14. Broecker, W.; Clark, E.; Hajdas, I.; Bonani, G. Glacial ventilation rates for the deep Pacific Ocean. *Paleoceanography* **2004**, *19*, PA2002. [[CrossRef](#)]
15. Broecker, W.; Clark, E. Search for a glacial-age ¹⁴C-depleted ocean reservoir. *Geophys. Res. Lett.* **2010**, *37*. [[CrossRef](#)]
16. Talley, L.D. Distribution and formation of North Pacific intermediate water. *J. Phys. Oceanogr.* **1993**, *23*, 517–537. [[CrossRef](#)]
17. Talley, L.; Nagata, Y.; Fujimura, M.; Iwao, T.; Kono, T.; Inagake, D.; Hirai, M.; Okuda, K. North Pacific Intermediate Water in the Kuroshio-Oyashio Mixed Water Region. *J. Phys. Oceanogr.* **1995**, *25*, 475–501. [[CrossRef](#)]
18. Kitani, K. An oceanographic study of the Okhotsk Sea - particularly in regard to cold waters. *Bull. Far East Fish. Res. Lab.* **1973**, *9*, 45–76.
19. Van Scoy, K.; Olson, D.B.; Fine, R.A. Ventilation of North Pacific Intermediate Water: The role of the Alaskan Gyre. *J. Geophys. Res.* **1991**, *96*, 16801–16810. [[CrossRef](#)]
20. Nakanowatari, T.; Ohshima, K.I.; Wakatsuchi, M. Warming and oxygen decrease of intermediate water in the northwestern North Pacific, originating from the Sea of Okhotsk, 1955–2004. *Geophys. Res. Lett.* **2007**, *34*, L04602. [[CrossRef](#)]
21. Feely, R.A.; Sabine, C.L.; Schlitzer, R.; Bullister, J.L.; Mecking, S.; Greeley, D. Oxygen utilization and organic carbon remineralization in the upper water column of the Pacific Ocean. *J. Oceanogr.* **2004**, *60*, 45–52. [[CrossRef](#)]
22. Deutsch, C.; Emerson, S.; Thompson, L. Fingerprints of climate change in North Pacific oxygen. *Geophys. Res. Lett.* **2005**, *32*, L16604. [[CrossRef](#)]
23. Deutsch, C.; Brix, H.; Ito, T.; Frenzel, H.; Thompson, L. Climate-Forced Variability of Ocean Hypoxia. *Science* **2011**, *333*, 336–339. [[CrossRef](#)] [[PubMed](#)]
24. Garcia, H.E.; Locarnini, R.A.; Boyer, T.P.; Antonov, J.I.; Baranova, O.K.; Zweng, M.M.; Johnson, D.R. *World Ocean Atlas 2009, Volume 3: Dissolved Oxygen, Apparent Oxygen Utilization, and Oxygen Saturation*; U.S. Government Printing Office: Washington, DC, USA, 2010; p. 344.

25. Sakamoto, T.; Ikehara, M.; Uchida, M.; Aoki, K.; Shibata, Y.; Kanamatsu, T.; Harada, N.; Iijima, K.; Katsuki, K.; Asahi, H. Millennial-scale variations of sea-ice expansion in the southwestern part of the Okhotsk Sea during the past 120 kyr: Age model and ice-rafted debris in IMAGES Core MD01-2412. *Glob. Planet. Chang.* **2006**, *53*, 58–77. [[CrossRef](#)]
26. Harada, N.; Ahagon, N.; Sakamoto, T.; Uchida, M.; Ikehara, M.; Shibata, Y. Rapid fluctuation of alkenone temperature in the southwestern Okhotsk Sea during the past 120 ky. *Glob. Planet. Chang.* **2006**, *53*, 29–46. [[CrossRef](#)]
27. Gorbarenko, S.A.; Psheneva, O.Y.; Artemova, A.V.; Matul, A.G.; Tiedemann, R.; Nuernberg, D. Paleoenvironment changes in the NW Okhotsk Sea for the last 18 kyr determined with micropaleontological, geochemical, and lithological data. *Deep Sea Res. Part I Oceanogr. Res. Pap.* **2010**, *57*, 797–811. [[CrossRef](#)]
28. Nürnberg, D.; Dethleff, D.; Tiedemann, R.; Kaiser, A.; Gorbarenko, S.A. Okhotsk Sea ice coverage and Kamchatka glaciation over the last 350 ka—Evidence from ice-rafted debris and planktonic $\delta^{18}\text{O}$. *Palaeogeogr. Palaeoclimatol. Palaeoecol.* **2011**, *310*, 191–205. [[CrossRef](#)]
29. Nürnberg, D.; Tiedemann, R. Environmental change in the Sea of Okhotsk during the last 1.1 million years. *Paleoceanography* **2004**, *19*, PA4011. [[CrossRef](#)]
30. Riethdorf, J.R.; Max, L.; Nürnberg, D.; Lembke-Jene, L.; Tiedemann, R. Deglacial history of (sub) sea surface temperatures and salinity in the subarctic NW Pacific: Implications for upper-ocean stratification. *Paleoceanography* **2013**, *28*, 91–104. [[CrossRef](#)]
31. Riethdorf, J.R. Late Pleistocene to Holocene Changes in Upper-Ocean Stratification and Its Impact on Marine Productivity, Sea Surface Temperatures, and Salinity in the Subarctic Northwest Pacific. Ph.D. Thesis, Christian-Albrechts-Universität zu Kiel, Kiel, Germany, 2012.
32. Ovsepyan, E.A.; Ivanova, E.V.; Max, L.; Riethdorf, J.R.; Nuernberg, D.; Tiedemann, R. Late quaternary oceanographic conditions in the Western Bering Sea. *Okeanologiya* **2013**, *53*, 211–222. [[CrossRef](#)]
33. Drysdale, R.N.; Hellstrom, J.C.; Zanchetta, G.; Fallick, A.E.; Goni, M.F.S.; Couchoud, I.; McDonald, J.; Maas, R.; Lohmann, G.; Isola, I. Evidence for Obliquity Forcing of Glacial Termination II. *Science* **2009**, *325*, 1527–1531. [[CrossRef](#)]
34. Knorr, G.; Lohmann, G. Southern Ocean origin for the resumption of Atlantic thermohaline circulation during deglaciation. *Nature* **2003**, *424*, 532–536. [[CrossRef](#)] [[PubMed](#)]
35. Knorr, G.; Lohmann, G.P. Rapid transitions in the Atlantic thermohaline circulation triggered by global warming and meltwater during the last deglaciation. *Geochem. Geophys. Geosyst.* **2007**, *8*. [[CrossRef](#)]
36. Lohmann, G. Atmospheric and oceanic freshwater transport during weak Atlantic overturning circulation. *Tellus Ser. A Dyn. Meteorol. Oceanogr.* **2003**, *55*, 438–449. [[CrossRef](#)]
37. Lohmann, G.; Lorenz, S. On the hydrological cycle under paleoclimatic conditions as derived from AGCM simulations. *J. Geophys. Res. Atmos.* **2000**, *105*, 17417–17436. [[CrossRef](#)]
38. Prange, M.; Romanova, V.; Lohmann, G. The glacial thermohaline circulation: Stable or unstable? *Geophys. Res. Lett.* **2002**, *29*. [[CrossRef](#)]
39. Romanova, V.; Prange, M.; Lohmann, G. Stability of the glacial thermohaline circulation and its dependence on the background hydrological cycle. *Clim. Dyn.* **2004**, *22*, 527–538. [[CrossRef](#)]
40. Kim, J.; Rimbu, N.; Lorenz, S.; Lohmann, G.; Nam, S.; Schouten, S.; Rühlemann, C.; Schneider, R. North Pacific and North Atlantic sea-surface temperature variability during the holocene. *Quat. Sci. Rev.* **2004**, *23*, 2141–2154. [[CrossRef](#)]
41. Kim, J.H.; Meggers, H.; Rimbu, N.; Lohmann, G.; Freudenthal, T.; Müller, P.J.; Schneider, R.R. Impacts of the North Atlantic gyre circulation on Holocene climate off northwest Africa. *Geology* **2007**, *35*, 387–390. [[CrossRef](#)]
42. Lorenz, S.J.; Lohmann, G. Acceleration technique for Milankovitch type forcing in a coupled atmosphere-ocean circulation model: Method and application for the Holocene. *Clim. Dyn.* **2004**, *23*, 727–743. [[CrossRef](#)]
43. Scholz, P.; Kieke, D.; Lohmann, G.; Ionita, M.; Rhein, M. Evaluation of Labrador Sea Water formation in a global Finite-Element Sea-Ice Ocean Model setup, based on a comparison with observational data. *J. Geophys. Res. Oceans* **2014**, *119*, 1644–1667. [[CrossRef](#)]
44. Rühlemann, C.; Mulitza, S.; Lohmann, G.; Paul, A.; Prange, M.; Wefer, G. Intermediate depth warming in the tropical Atlantic related to weakened thermohaline circulation: Combining paleoclimate data and modeling results for the last deglaciation. *Paleoceanography* **2004**, *19*. [[CrossRef](#)]

45. Lohmann, G.; Wackerbarth, A.; Langebroek, P.M.; Werner, M.; Fohlmeister, J.; Scholz, D.; Mangini, A. Simulated European stalagmite record and its relation to a quasi-decadal climate mode. *Clim. Past* **2013**, *9*, 89–98. [[CrossRef](#)]
46. Felis, T.; Lohmann, G.; Kuhnert, H.; Lorenz, S.J.; Scholz, D.; Patzold, J.; Al-Rousan, S.A.; Al-Moghrabi, S.M. Increased seasonality in Middle East temperatures during the last interglacial period. *Nature* **2004**, *429*, 164–168. [[CrossRef](#)] [[PubMed](#)]
47. Rimbu, N.; Lohmann, G.; Grosfeld, K. Northern Hemisphere atmospheric blocking in ice core accumulation records from northern Greenland. *Geophys. Res. Lett.* **2007**, *34*, 5. [[CrossRef](#)]
48. Rimbu, N.; Lohmann, G.; Felis, T.; Patzold, J. Arctic oscillation signature in a Red Sea coral. *Geophys. Res. Lett.* **2001**, *28*, 2959–2962. [[CrossRef](#)]
49. Dima, M.; Lohmann, A. Fundamental and derived modes of climate variability: Concept and application to interannual time-scales. *Tellus Ser. A Dyn. Meteorol. Oceanogr.* **2004**, *56*, 229–249. [[CrossRef](#)]
50. Leduc, G.; Schneider, R.; Kim, J.H.; Lohmann, G. Holocene and Eemian sea surface temperature trends as revealed by alkenone and Mg/Ca paleothermometry. *Quat. Sci. Rev.* **2010**, *29*, 989–1004. [[CrossRef](#)]
51. Lohmann, G.; Pfeiffer, M.; Laepple, T.; Leduc, G.; Kim, J.H. A model-data comparison of the Holocene global sea surface temperature evolution. *Clim. Past* **2013**, *9*, 1807–1839. [[CrossRef](#)]
52. Butzin, M.; Prange, M.; Lohmann, G. Radiocarbon simulations for the glacial ocean: The effects of wind stress, Southern Ocean sea ice and Heinrich events. *Earth Planet. Sci. Lett.* **2005**, *235*, 45–61. [[CrossRef](#)]
53. Butzin, M.; Lohmann, G.P.; Bickert, T. Miocene ocean circulation inferred from marine carbon cycle modeling combined with benthic isotope records. *Paleoceanography* **2011**, *26*, PA1203. [[CrossRef](#)]
54. Herold, M.; Lohmann, G. Eemian tropical and subtropical African moisture transport: An isotope modelling study. *Clim. Dyn.* **2009**, *33*, 1075–1088. [[CrossRef](#)]
55. Werner, M.; Langebroek, P.M.; Carlsen, T.; Herold, M.; Lohmann, G. Stable water isotopes in the ECHAM5 general circulation model: Toward high-resolution isotope modeling on a global scale. *J. Geophys. Res. Atmos.* **2011**, *116*, D15109. [[CrossRef](#)]
56. Xu, X.; Werner, M.; Butzin, M.; Lohmann, G. Water isotope variations in the global ocean model MPI-OM. *Geosci. Model Dev.* **2012**, *5*, 809–818. [[CrossRef](#)]
57. Laepple, T.; Werner, M.; Lohmann, G.P. Synchronicity of Antarctic temperatures and local solar insolation on orbital timescales. *Nature* **2011**, *471*, 91–94. [[CrossRef](#)] [[PubMed](#)]
58. Broecker, W. Glacial to Interglacial Changes in Ocean Chemistry. *Prog. Oceanogr.* **1982**, *11*, 151–197. [[CrossRef](#)]
59. Boyle, E.A. Vertical oceanic nutrient fractionation and glacial/interglacial CO₂ cycles. *Nat. News* **1988**, *331*, 55–56. [[CrossRef](#)]
60. Mix, A.C.; Pisias, N.G.; Zahn, R.; Rugh, W.; Lopez, C.; Nelson, K. Carbon 13 in Pacific Deep and Intermediate Waters, 0–370 ka: Implications for Ocean Circulation and Pleistocene CO₂. *Paleoceanography* **1991**, *6*, 205–226. [[CrossRef](#)]
61. Zahn, R.; Pedersen, T.F.; Bornhold, B.D.; Mix, A.C. Water Mass Conversion in the Glacial Subarctic Pacific (54° N, 148° W): Physical Constraints and the Benthic-Planktonic Stable Isotope Record. *Paleoceanography* **1991**, *6*, 543–560. [[CrossRef](#)]
62. Keigwin, L. Glacial-age hydrography of the far northwest Pacific Ocean. *Paleoceanography* **1998**, *13*, 323–339. [[CrossRef](#)]
63. Ohkushi, K.; Itaki, T.; Nemoto, N. Last Glacial-Holocene change in intermediate-water ventilation in the Northwestern Pacific. *Quat. Sci. Rev.* **2003**, *22*, 1477–1484. [[CrossRef](#)]
64. Matsumoto, K.; Oba, T.; Lynch-Stieglitz, J.; Yamamoto, H. Interior hydrography and circulation of the glacial Pacific Ocean. *Quat. Sci. Rev.* **2002**, *21*, 1693–1704. [[CrossRef](#)]
65. Herguera, J.C.; Herbert, T.; Kashgarian, M.; Charles, C. Intermediate and deep water mass distribution in the Pacific during the Last Glacial Maximum inferred from oxygen and carbon stable isotopes. *Quat. Sci. Rev.* **2010**, *29*, 1228–1245. [[CrossRef](#)]
66. Ahagon, N.; Ohkushi, K.; Uchida, M.; Mishima, T. Mid-depth circulation in the northwest Pacific during the last deglaciation: Evidence from foraminiferal radiocarbon ages. *Geophys. Res. Lett.* **2003**, *30*, 2097. [[CrossRef](#)]
67. Harada, N.; Ahagon, N.; Uchida, M.; Murayama, M. Northward and southward migrations of frontal zones during the past 40 kyr in the Kuroshio-Oyashio transition area. *Geochem. Geophys. Geosyst.* **2004**, *5*, Q09004. [[CrossRef](#)]

68. Okazaki, Y.; Timmermann, A.; Menviel, L.; Harada, N.; Abe-Ouchi, A.; Chikamoto, M.O.; Mouchet, A.; Asahi, H. Deepwater formation in the North Pacific during the Last Glacial Termination. *Science* **2010**, *329*, 200–204. [[CrossRef](#)]
69. Kienast, S.; Hendy, I.; Crusius, J.; Pedersen, T.; Calvert, S. Export production in the subarctic North Pacific over the last 800 kyrs: No evidence for iron fertilization? *J. Oceanogr.* **2004**, *60*, 189–203. [[CrossRef](#)]
70. Brunelle, B.G.; Sigman, D.M.; Jaccard, S.L.; Keigwin, L.D.; Plessen, B.; Schettler, G.; Cook, M.S.; Haug, G.H. Glacial/interglacial changes in nutrient supply and stratification in the western subarctic North Pacific since the penultimate glacial maximum. *Quat. Sci. Rev.* **2010**, *29*, 2579–2590. [[CrossRef](#)]
71. Kiefer, T.; Kienast, M. Patterns of deglacial warming in the Pacific Ocean: A review with emphasis on the time interval of Heinrich event 1. *Quat. Sci. Rev.* **2005**, *24*, 1063–1081. [[CrossRef](#)]
72. Sarnthein, M.; Kiefer, T.; Grootes, P.; Elderfield, H.; Erlenkeuser, H. Warmings in the far northwestern Pacific promoted pre-Clovis immigration to America during Heinrich event 1. *Geology* **2006**, *34*, 141–144. [[CrossRef](#)]
73. Sarnthein, M.; Grootes, P.M.; Kennett, J.P.; Nadeau, M.; Schmittner, A.; Chiang, J.; Hemming, S. 14C Reservoir Ages Show Deglacial Changes in Ocean Currents and Carbon Cycle. In *Ocean Circulation: Mechanisms and Impacts*, AGU Geophysical Monograph Series; Schmittner, A., Chiang, J.C.H., Hemming, S.R., Eds.; American Geophysical Union: Washington, DC, USA, 2007; Volume 173, pp. 175–196.
74. Chikamoto, M.O.; Menviel, L.; Abe-Ouchi, A.; Ohgaito, R.; Timmermann, A.; Okazaki, Y.; Harada, N.; Oka, A.; Mouchet, A. Variability in North Pacific intermediate and deep water ventilation during Heinrich events in two coupled climate models. *Deep Sea Res. Part II Top. Stud. Oceanogr.* **2012**, *61–64*, 114–126. [[CrossRef](#)]
75. Jaccard, S.L.; Galbraith, E. Direct ventilation of the North Pacific did not reach the deep ocean during the last deglaciation. *Geophys. Res. Lett.* **2013**, *40*, 199–203. [[CrossRef](#)]
76. Jaccard, S.L.; Galbraith, E.D. Large climate-driven changes of oceanic oxygen concentrations during the last deglaciation. *Nat. Geosci.* **2011**, *5*, 151–156. [[CrossRef](#)]
77. Zheng, Y.; Van Geen, A.; Anderson, R.; Gardner, J.; Dean, W. Intensification of the northeast Pacific oxygen minimum zone during the Bolling-Allerod warm period. *Paleoceanography* **2000**, *15*, 528–536. [[CrossRef](#)]
78. Crusius, J.; Pedersen, T.; Kienast, S.; Keigwin, L.; Labeyrie, L. Influence of northwest Pacific productivity on North Pacific Intermediate Water oxygen concentrations during the Bøling-Ållerød interval (14.7–12.9 ka). *Geology* **2004**, *32*, 633–636. [[CrossRef](#)]
79. Lam, P.J.; Robinson, L.F.; Blusztajn, J.; Li, C.; Cook, M.S.; McManus, J.F.; Keigwin, L.D. Transient stratification as the cause of the North Pacific productivity spike during deglaciation. *Nat. Geosci.* **2013**, *6*, 622–626. [[CrossRef](#)]
80. Rasmussen, S.; Andersen, K.; Svensson, A.; Steffensen, J.; Vinther, B.; Clausen, H.; Siggaard-Andersen, M.; Johnsen, S.; Larsen, L.; Dahl-Jensen, D.; et al. A new Greenland ice core chronology for the last glacial termination. *J. Geophys. Res. Atmos.* **2006**, *111*, D06102. [[CrossRef](#)]
81. Max, L.; Riethdorf, J.-R.; Tiedemann, R.; Smirnova, M.; Lembke-Jene, L.; Fahl, K.; Nürnberg, D.; Matul, A.; Mollenhauer, G. Sea surface temperature variability and sea-ice extent in the subarctic northwest Pacific during the past 15,000 years. *Paleoceanography* **2012**, *27*, PA3213. [[CrossRef](#)]
82. Waelbroeck, C.; Labeyrie, L.; Michel, E.; Duplessy, J.C.; McManus, J.F.; Lambeck, K.; Balbon, E.; Labracherie, M. Sea-level and deep water temperature changes derived from benthic foraminifera isotopic records. *Quat. Sci. Rev.* **2002**, *21*, 295–305. [[CrossRef](#)]
83. Kuroyanagi, A.; Kawahata, H.; Nishi, H. Seasonal variation in the oxygen isotopic composition of different-sized planktonic foraminifer *Neogloboquadrina pachyderma* (sinistral) in the northwestern North Pacific and implications for reconstruction of the paleoenvironment. *Paleoceanography* **2011**, *26*. [[CrossRef](#)]
84. Kuroyanagi, A.; Kawahata, H.; Nishi, H.; Honda, M.C. Seasonal to interannual changes in planktonic foraminiferal assemblages in the northwestern North Pacific: Sediment trap results encompassing a warm period related to El Niño. *Palaeoogeogr. Palaoclimatol. Palaeoecol.* **2008**, *262*, 107–127. [[CrossRef](#)]
85. Kuroyanagi, A.; Kawahata, H.; Narita, H.; Ohkushi, K.; Aramaki, T. Reconstruction of paleoenvironmental changes based on the planktonic foraminiferal assemblages off Shimokita (Japan) in the northwestern North Pacific. *Glob. Planet. Chang.* **2006**, *53*, 92–107. [[CrossRef](#)]
86. Kuroyanagi, A.; Kawahata, H. Vertical distribution of living planktonic foraminifera in the seas around Japan. *Mar. Micropaleontol.* **2004**, *53*, 173–196. [[CrossRef](#)]
87. Bauch, D.; Erlenkeuser, H.; Winckler, G.; Pavlova, G.; Thiede, J. Carbon isotopes and habitat of polar planktic foraminifera in the Okhotsk Sea: The ‘carbonate ion effect’ under natural conditions. *Mar. Micropaleontol.* **2002**, *45*, 83–99. [[CrossRef](#)]

88. Méheust, M.; Fahl, K.; Stein, R. Variability in modern sea surface temperature, sea ice and terrigenous input in the sub-polar North Pacific and Bering Sea: Reconstruction from biomarker data. *Org. Geochem.* **2013**, *57*, 54–64. [[CrossRef](#)]
89. Müller, J.; Wagner, A.; Fahl, K.; Stein, R.; Prange, M.; Lohmann, G. Towards quantitative sea ice reconstructions in the northern North Atlantic: A combined biomarker and numerical modelling approach. *Earth Planet. Sci. Lett.* **2011**, *306*, 137–148. [[CrossRef](#)]
90. Bonnet, S.; de Vernal, A.; Gersonde, R.; Lembke-Jene, L. Modern distribution of dinocysts from the North Pacific Ocean (37–64° N, 144° E–148° W) in relation to hydrographic conditions, sea-ice and productivity. *Mar. Micropaleontol.* **2012**, *84–85*, 87–113. [[CrossRef](#)]
91. Jungclauss, J.H.; Keenlyside, N.; Botzet, M.; Haak, H.; Luo, J.J.; Latif, M.; Marotzke, J.; Mikolajewicz, U.; Roeckner, E.; Jungclauss, J.H.; et al. Ocean Circulation and Tropical Variability in the Coupled Model ECHAM5/MPI-OM. *J. Clim.* **2006**, *19*, 3952–3972. [[CrossRef](#)]
92. Knorr, G.; Butzin, M.; Micheels, A.; Lohmann, G. A warm Miocene climate at low atmospheric CO₂ levels. *Geophys. Res. Lett.* **2011**, *38*. [[CrossRef](#)]
93. Stepanek, C.; Lohmann, G.P. Modelling mid-Pliocene climate with COSMOS. *Geosci. Model Dev.* **2012**, *5*, 1221–1243. [[CrossRef](#)]
94. Dowsett, H.J.; Foley, K.M.; Stoll, D.K.; Chandler, M.A.; Sohl, L.E.; Bentsen, M.; Otto-Bliesner, B.L.; Bragg, F.J.; Chan, W.L.; Contoux, C.; et al. Sea Surface Temperature of the mid-Piacenzian Ocean: A Data-Model Comparison. *Sci. Rep.* **2013**, *3*, 2013. [[CrossRef](#)]
95. Kageyama, M.; Merkel, U.; Otto-Bliesner, B.; Prange, M.; Abe-Ouchi, A.; Lohmann, G.; Ohgaito, R.; Roche, D.M.; Singarayer, J.; Swingedouw, D.; et al. Climatic impacts of fresh water hosing under Last Glacial Maximum conditions: A multi-model study. *Clim. Past* **2013**, *9*, 935–953. [[CrossRef](#)]
96. Gong, X.; Knorr, G.; Lohmann, G.P.; Zhang, X. Dependence of abrupt Atlantic meridional ocean circulation changes on climate background states. *Geophys. Res. Lett.* **2013**, *40*, 3698–3704. [[CrossRef](#)]
97. Wei, W.; Lohmann, G. Simulated Atlantic Multidecadal Oscillation during the Holocene. *J. Clim.* **2012**, *25*, 6989–7002. [[CrossRef](#)]
98. Varma, V.; Prange, M.; Merkel, U.; Kleinen, T.; Lohmann, G.P.; Pfeiffer, M.; Renssen, H.; Wagner, A.; Wagner, S.; Schulz, M. Holocene evolution of the Southern Hemisphere westerly winds in transient simulations with global climate models. *Clim. Past* **2012**, *8*, 391–402. [[CrossRef](#)]
99. Hibler, W.D. Dynamic Thermodynamic Sea Ice Model. *J. Phys. Oceanogr.* **1979**, *9*, 815–846. [[CrossRef](#)]
100. Scholz, P.; Lohmann, G.; Wang, Q.; Danilov, S. Evaluation of a Finite-Element Sea-Ice Ocean Model (FESOM) set-up to study the interannual to decadal variability in the deep-water formation rates. *Ocean Dyn.* **2013**, *63*, 347–370. [[CrossRef](#)]
101. Hesse, T.; Butzin, M.; Bickert, T.; Lohmann, G. A model-data comparison of $\delta^{13}\text{C}$ in the glacial Atlantic Ocean. *Paleoceanography* **2011**, *26*, PA3220. [[CrossRef](#)]
102. Mikolajewicz, U.; Crowley, T.J.; Schiller, A.; Voss, R. Modelling teleconnections between the North Atlantic and North Pacific during the Younger Dryas. *Nature* **1997**, *387*, 384–387. [[CrossRef](#)]
103. Vellinga, M.; Wood, R.A. Global climatic impacts of a collapse of the Atlantic thermohaline circulation. *Clim. Chang.* **2002**, *54*, 251–267. [[CrossRef](#)]
104. Dietrich, S.; Werner, M.; Spanghel, T.; Lohmann, G. Influence of orbital forcing and solar activity on water isotopes in precipitation during the mid- and late Holocene. *Clim. Past* **2013**, *9*, 13–26. [[CrossRef](#)]
105. Saenko, O.; Schmittner, A.; Weaver, A. The Atlantic-Pacific seesaw. *J. Clim.* **2004**, *17*, 2033–2038. [[CrossRef](#)]
106. Schmittner, A.; Galbraith, E.D.; Hostetler, S.W.; Pedersen, T.F.; Zhang, R. Large fluctuations of dissolved oxygen in the Indian and Pacific oceans during Dansgaard-Oeschger oscillations caused by variations of North Atlantic Deep Water subduction. *Paleoceanography* **2007**, *22*, PA3207. [[CrossRef](#)]
107. Yang, X.; DelSole, T. Systematic Comparison of ENSO Teleconnection Patterns between Models and Observations. *J. Clim.* **2012**, *25*, 425–446. [[CrossRef](#)]

